Polyoxometalates

Reversible Redox Reactions in an Extended Polyoxometalate Framework Solid**

Chris Ritchie, Carsten Streb, Johannes Thiel, Scott G. Mitchell, Haralampos N. Miras, De-Liang Long, Thomas Boyd, Robert D. Peacock, Thomas McGlone, and Leroy Cronin

Extended modular frameworks that incorporate inorganic building blocks represent a new field of research where "active sites" can be engineered to respond to guest inclusion.[1–2] This process can initiate highly specific chemical reactions[3] that switch the overall nature of the framework, and it may even be developed to facilitate directed chemical reactions similar to those found in enzymatic systems. Achievement of this degree of sophistication requires the ability to control the framework assembly as precisely as in metal–organic frameworks,[1,4–6] combined with the stability and functionality of inorganic zeolites and related systems.[7] Although progress has been made in fine-tuning the reactivity of framework materials,[8] reversible redox single-crystal to single-crystal (SC–SC) transformations that retain long-range order have not yet been observed.[9] Thus, it can be suggested that the best way to engineer redox- and electronically active frameworks would be to incorporate building blocks based on polyoxometalate (POM) clusters,[10–12] constructed from $\{MO_x\}$ units where M = Mo, W, V, Nb and $x = 4$–7. These clusters are attractive units for the construction of such frameworks since they are highly redox active and can incorporate a range of main-group-templating $\{XO_n\}$ units, as exemplified by the Keggin ion $[M_{12}O_{36}X^mO_4]^{n-}$. This ion can incorporate anions such as phosphate and silicate, and can bind transition metals within structural vacancies.[13]

Herein we show that the directed assembly of a pure metal oxide framework, $[(C_4H_{10}NO)_{40}(W_{72}M_{12}O_{268}X_7)_n]$ (M = Mn^{III}, X = Si, $\mathbf{1_{ox}}$),[14] based upon substituted Keggin-type POM building blocks, yields a material that can undergo a reversible redox process that involves the simultaneous inclusion of the redox reagent with a concerted and spatially ordered redox change of the framework. Compound $\mathbf{1_{ox}}$ can also be repeatedly disassembled into its building blocks by dissolution in hot water; subsequent recrystallization results in the reassembly of unmodified $\mathbf{1_{ox}}$. These unique properties mean that this compound defines a new class of materials that bridges the gap between coordination compounds, metal–

organic frameworks, and solid-state oxides. Furthermore, it has been shown that all the manganese(III) centers in $\mathbf{1_{ox}}$ can be "switched" to manganese(II) using a suitable reducing agent to give the fully reduced framework $\mathbf{1_{red}}$. The redox process occurs with retention of long-range order by cooperative structural changes within the W-O-Mn linkages that connect the Keggin units. The nature of the redox process can be precisely deduced because of the SC–SC transformation between the oxidized and reduced states of the framework. This is important as, until now, covalently connected 3D polyoxometalate-based frameworks with large pockets (greater than 10 Å) could be assembled only by the addition of "bridging" electrophiles. However, these solids typically have low stabilities and are not amenable to systematic design strategies, for instance the introduction of redox switchability.

The approach adopted here involves the reaction of the divacant lacunary polyoxometalate $[\gamma\text{-}SiW_{10}O_{36}]^{8-}$ [15] with manganese(II) in the presence of morpholinium cations and potassium permanganate, under strict pH control, to yield $\mathbf{1_{ox}}$, which has the composition $[(C_4H_{10}NO)_{40}(W_{72}Mn^{III}_{12}O_{268}Si_7)_n]\cdot 48\,H_2O$. Compound $\mathbf{1_{ox}}$ crystallizes[16] in the cubic space group $I\bar{4}3d$ and has a unit cell of $a = 38.5$ Å with a unit cell volume of 57249 Å^3. The metal oxide framework encloses elliptical pockets of $26.85 \times 23.62 \times 12.93$ Å which house solvent molecules and morpholinium cations. Therefore $\mathbf{1_{ox}}$ is the prototype of a 3D polyoxometalate framework that is based on pure metal oxides and constructed without the use of external linkers[17] to connect the polyanionic framework nodes. The assembly of $\mathbf{1_{ox}}$ is achieved by the use of metastable heteropolytungstate ions that are connected directly by W-O-M units where M is a first-row transition metal.[15,18] Here we designate the structure of $\mathbf{1_{ox}}$ as POM-1; the structure type comprises a unit cell in which four 3-connected and three 4-connected Keggin clusters are cross-linked into an infinite 3D framework (see Figure 1).

Unlike any other 3D polyoxometalate network material reported to date, the POM-1 framework is composed solely of cluster anions that are directly connected by symmetry-equivalent W-O-M linkages over which the tungsten and manganese atoms are statistically disordered with an average metal–oxygen bond length of 1.822 Å (for $\mathbf{1_{ox}}$). The structure of this material can therefore be described as an infinite array of 3- and 4-connected Keggin polyanions, where each three-connected unit is surrounded by three neighboring clusters in a trigonal-planar fashion, and each 4-connected unit features four nearest neighbors located on the vertices of a distorted tetrahedron (see Figure 1). Conceptually, the nodes of the framework can be considered as an equal distribution of tetravacant $\{SiW_8O_{36}\}$ (**W8**) and trivacant $\{SiW_9O_{37}\}$ (**W9**)

[*] Dr. C. Ritchie, Dr. C. Streb, J. Thiel, S. G. Mitchell, Dr. H. N. Miras, Dr. D.-L. Long, T. Boyd, R. D. Peacock, T. McGlone, Prof. L. Cronin
WestCHEM, Department of Chemistry
The University of Glasgow
University Avenue, Glasgow G12 8QQ, Scotland (UK)
Fax: (+44) 141-330-4888
E-mail: l.cronin@chem.gla.ac.uk
Homepage: http://www.chem.gla.ac.uk/staff/lee/

Supporting information for this article is available on the WWW under http://dx.doi.org/10.1002/anie.200802594.
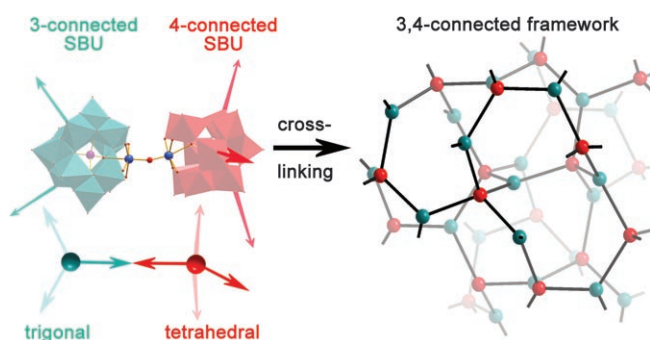
Figure 1. Rationalization of the POM-1 framework found in compound **1**. The network is built from two types of lacunary Keggin clusters which act as either trigonal (green) or tetrahedral nodes (red). The polyhedral representation of the clusters (top left) more clearly shows how the secondary building units (SBUs) are linked into an infinite 3D framework based upon 3-connected and 4-connected clusters. The nodal connectivity is shown on the right.

units which are subsequently cross-linked by [W-O-Mn] bridges, which effectively "bolt" together the nodal units. Considering the statistical disorder of the tungsten and manganese atoms and the substitution pattern described above, this results in a formal assignment of 1.5 manganese and 1.5 tungsten atoms to every trivacant cluster, with each tetravacant building block supporting two manganese and two tungsten atoms. Formally, the general framework description $\{W_{72}Mn_{12}\}$ can thus be rationalized as $\{(MnW)_{3/2}\subset\mathbf{W9}\}_4$-$\{(MnW)_{4/2}\subset\mathbf{W8}\}_3$ (see Figure 2).

The framework is topologically identical to that of cubic germanium nitride which also crystallizes in the space group $I\bar{4}3d$. This material has the formula Ge_3N_4, with the germanium atoms acting as tetrahedral nodes and the nitrogen

atoms as trigonal nodes.[19] It is therefore reasonable to compare the structural features of this material to the family of POM-1 clusters since this illustrates the effect of replacing atomic nodes in classical materials with nanosized clusters. This polymorph of intrinsically neutral germanium nitride has a close-packed structure, with no additional solvent molecules or ligands in the crystal lattice. One striking feature, however, is the formation of puckered eight-membered rings that are composed of four germanium atoms and four nitrogen atoms throughout the structure. These ellipsoidal rings in Ge_3N_4 have a circumference of 14.88 Å, with approximate atom-to-atom dimensions of 2.97 Å × 4.61 Å. In comparison, the topologically equivalent eight-membered rings in $\mathbf{1_{ox}}$ are composed of four 3-connected and four 4-connected clusters and have a circumference of approximately 92.5 Å, measured by taking the shortest route through the cluster heteroatoms. This drastic increase in circumference results in ellipsoidal rings with dimensions of 9.45 Å × 12.93 Å. Further extrapolation of the framework reveals the formation of ten-membered rings, which are capped above and below the plane by two additional cluster units resulting in the formation of a cavity with nanoscale dimensions of 2.7 × 2.4 × 1.3 nm, with four eight-membered rings leading into this cage (see Figure 2). These internal pockets accommodate the charge-balancing counterions along with a significant number of water molecules of crystallization and represent 69 % of the unit cell volume as shown by the yellow ellipse in Figure 2.

Experiments in which ascorbic acid was employed as a selective reducing agent revealed a reversible SC–SC redox reaction with reduction of all manganese(III) centers in $\mathbf{1_{ox}}$ to manganese(II) in $\mathbf{1_{red}}$ whilst the framework integrity of POM-1 was completely retained (see Figure 3). The redox process can be broken down into three distinct steps where first the ascorbic acid diffuses into the framework of POM-1 and occupies the internal pockets described above. Subsequent electron transfer to the manganese(III) centers occurs within this "active site" where the manganese(III) ions are exposed to the pore walls and are accessible for electron transfer. During this redox process, the ascorbic acid is oxidized to dehydroascorbic acid and subsequently forms a 2-methyl hemiketal (see Figure 3).[20] Finally, this oxidation product is released into solution where it can be detected by ^{1}H NMR spectroscopy (Figure S3 in the Supporting Information). The reduction of the manganese centers was directly observed using solid-state UV/Vis spectroscopy, which shows a manganese(III) absorption peak at $\lambda_{max} = 480$ nm for $\mathbf{1_{ox}}$ and two absorption maxima at $\lambda_{max1} = 350$ nm and $\lambda_{max2} = 373$ nm, confirming the presence of manganese(II) in compound $\mathbf{1_{red}}$. Furthermore, no absorption was detected in the region characteristic of reduced tungsten centers. The complete reduction was confirmed by a redox titration that showed that all manganese centers in compound $\mathbf{1_{red}}$ are in the $+2$ oxidation state.

The redox switching of the metal oxide framework in POM-1 was investigated using single-crystal X-ray diffraction of compounds $\mathbf{1_{ox}}$ and $\mathbf{1_{red}}$. The study revealed that the principal framework connectivity remained intact after reduction, which allowed a detailed investigation of the
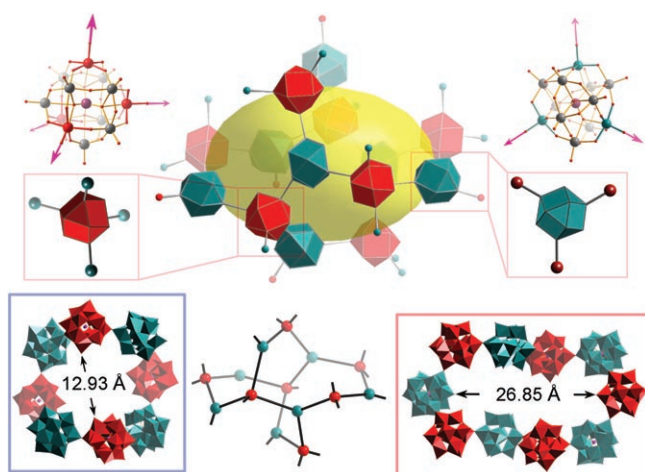

Figure 2. Illustration of the nanosized pockets in POM-1 (top center) highlighted by the yellow ellipsoid (dimensions: 2.7 × 2.4 × 1.3 nm). The 3- and 4-connected Keggin clusters (green and red, respectively) demonstrate the connectivity of each unit. The trigonal and tetrahedral building block connectors are shown on the top right and left; respectively; purple arrows highlight the connecting modes. A schematic view of the internal pocket is illustrated at the bottom center. The polyhedral representation of the eight-membered ring (bottom left) and of the ten-membered ring (bottom right) illustrates the smallest and largest dimensions of the pocket.
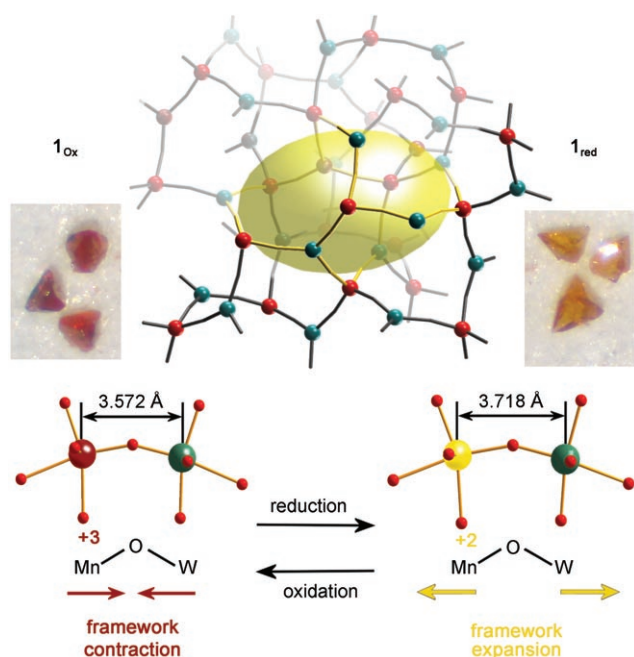
Figure 3. Schematic illustration of the SC–SC redox transformation from 1_{ox} to 1_{red}. The framework of POM-1 (top center; 3-connected nodes: green, 4-connected nodes: red, internal void: yellow ellipsoid) can be reversibly "switched" from a fully oxidized state (1_{ox}, left) to a fully reduced state (1_{red}, right) under framework expansion from a unit cell volume of 57 249 $Å^3$ to 60 386 $Å^3$. The photographic inserts illustrate the change in crystal color from the oxidized form (1_{ox}, red-brown) to the reduced form (1_{red}, light yellow). The switching process is complete for both 1_{ox} to 1_{red} and 1_{red} to 1_{ox} within 60 min when the concentration of the ascorbic acid and *m*CPBA is 10 mм.

changes triggered by the redox process. The asymmetric unit of POM-1 contains only five unique tungsten(VI) centers, three of which are located in the 3-connected node and two in the 4-connected Keggin. All the metal centers have the anticipated octahedral geometry with a typically short bond to the terminal oxido ligand (average $d_{W=O} = 1.662$ Å). On reduction of 1_{ox} to yield 1_{red}, the selective reduction of the manganese(III) centers to manganese(II) can be observed crystallographically by the increase in the size of the unit cell axes from 38.514(5) to 39.233(1) Å (a change of approximately 0.719 Å, 1.87 %) and the consequent increase in unit cell volume from 57 249 $Å^3$ to 60 386 $Å^3$ (a change of 3137 $Å^3$, 5.48 %; see Figure 3). This volume change is related to the oxidation state change of the manganese center upon reduction and the simultaneous expansion of the Mn-O-W linkages shown by the change of the Mn···W distance from 3.572(3) Å in 1_{ox} to 3.718(3) Å in 1_{red}. Furthermore, the reversibility of this redox switching was demonstrated by reoxidation of the framework from 1_{red} to 1_{ox} using *meta*-chloroperoxybenzoic acid (*m*CPBA) over at least three consecutive cycles. Single-crystal X-ray studies of the reoxidized material demonstrate the retention of the framework structure. The reversible redox switching was followed by solid-state and solution UV spectroscopy, confirming that the reaction proceeds by a one-electron reduction of manganese-

(III) to manganese(II) with subsequent reoxidation to manganese(III). The reaction can also be followed visually as the crystal color changes from deep red-brown in 1_{ox} to light yellow in 1_{red} (see Figure 3). The transformation is therefore unambiguously supported by all the crystallographic, spectroscopic, and analytical studies showing that the framework can be fully "switched" between a reduced and oxidized state.

The unprecedented ability of such a robust framework material to be recrystallized from hot aqueous solution complements the solid-state stability and tunable redox properties of 1_{ox}. Indeed, this characteristic highlights the dramatic variation in physical properties that can be achieved through the use of stable polyoxometalate building blocks for the formation of metal oxide framework materials, with the hydrophilic nature of the clusters facilitating the disassembly of the framework units and subsequent solubilization. The self-assembly process is repeated upon cooling and 1_{ox} is reformed. In addition, disassembly of 1_{red} results in the reoxidation of the building blocks in solution, and 1_{ox} is subsequently regenerated and recrystallized. Such a property is highly desirable, not only for purification purposes but as a potential separation method for contaminated materials and for functional materials that can undergo electronic and phase state changes (see Figure 4).
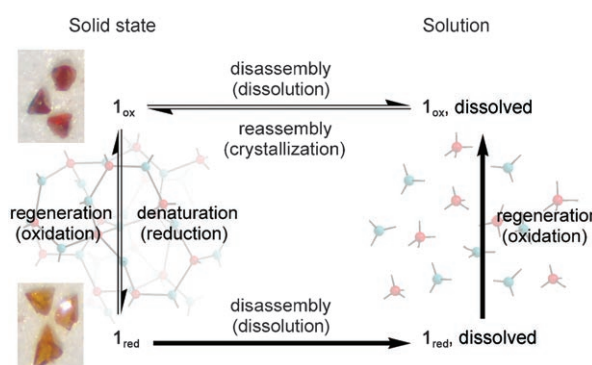

Figure 4. Schematic representation of the possible transformations between 1_{ox} and 1_{red} in the solid state and by dissolution and recrystallization from hot aqueous solution. 1_{ox} can be reversibly reduced to give 1_{red} in the solid state (left). 1_{red} can be irreversibly disassembled into its building blocks by dissolution (bottom), subsequent oxidation of the manganese centers results in the regeneration of the building blocks of 1_{ox} in solution (right). Recrystallization of the solution results in the reassembly of 1_{ox}.

In conclusion, compound **1** represents the first example of a pure Keggin network $[\{W_{72}M_{12}O_{268}X_7\}_n]^{y-}$. A similar synthetic strategy which employs other metal ions (M) and heterotemplates (X) should result in the formation of a family of related POM-1 materials. The combination of the crystallographically conserved redox switching and the ability to reform the material by repeated dissolution and recrystallization underlines its unique nature, offering a great deal of potential for investigations of this new type of functional and responsive material.

Communications

Experimental Section

1_{ox}: Morpholine (9.0 g, 103 mmol) was added to 1 M NaCl (200 mL) and the pH was subsequently adjusted to 8.0 by addition of 4.5 M H$_2$SO$_4$. At this point fresh air-dried K$_8$SiW$_{10}$O$_{36}$·12H$_2$O (1.486 g, 0.50 mmol) was added under vigorous stirring until fully dissolved. Solid MnSO$_4$·H$_2$O (127 mg, 0.75 mmol) was then added, resulting in a bright yellow solution, and the pH was adjusted to 7.80 by addition of 4.5 M H$_2$SO$_4$. KMnO$_4$ (24 mg, 0.15 mmol) was then added slowly and the solution was stirred for a further 5 min. At this point a deep-brown solution was obtained which was then centrifuged to remove any insoluble material. Finally the pH of the solution was adjusted to 7.75 by addition of 4.5 M H$_2$SO$_4$. Tetrahedral crystals of a quality suitable for diffraction began to form after two weeks. Yield after one month: 350 mg (15.4 µmol, 22.12% based on W). Elemental analysis calcd (%) for (C$_4$H$_{10}$NO)$_{40}$[W$_{72}$Mn$_{12}$O$_{268}$Si$_7$]·48H$_2$O, C$_{160}$H$_{496}$N$_{40}$Mn$_{12}$O$_{356}$Si$_7$W$_{72}$, M_w = 22770 g mol^{-1}: C 8.44, H 2.20, N 2.46, W 58.13, Mn 2.90; found: C 8.79, H 2.16, N 2.50, W 58.01, Mn 2.95. FTIR (KBr) $\tilde{v}$ = 1635(m), 1453(sh), 1310(sh), 1102(sh), 1042(sh), 984(sh), 900(sh), 737(br) cm^{-1}. UV/Vis (H$_2$O): λ_{max} (ε) = 480 nm (2.38 × 10^4).

1_{red}: Air-dried 1_{ox} (20 mg, 0.88 µmol) was added to MeOH (5 mL) in which it was completely insoluble. L-Ascorbic acid (10 mg, 56.8 µmol) was then added which dissolved over the course of a few minutes. Within 60 min the reduction of manganese(III) to manganese(II) in 1_{ox} was complete with retention of the crystallinity of the material resulting in the SC–SC transformation and generation of 1_{red}. This transformation was confirmed by collection of a second single-crystal data set which showed elongation of the [W-O-Mn] distances in accordance with reduction of manganese(III) to manganese(II). Elemental analysis calcd (%) for (C$_4$H$_{10}$NO)$_{40}$H$_{12}$-[W$_{72}$Mn$_{12}$O$_{268}$Si$_7$]·48H$_2$O, C$_{160}$H$_{508}$Mn$_{12}$N$_{40}$O$_{356}$Si$_7$W$_{72}$, M_w = 22782 g mol^{-1}: C 8.44, H 2.20, N 2.46, W 58.13, Mn 2.90; found: C 8.94, H 2.38, N 2.42, W 55.00, Mn 2.81. The increase in carbon content is most likely associated with the uptake of L-ascorbic acid into the structural voids. FTIR (KBr) $\tilde{v}$ = 2939(s), 2849(s), 1599(wk), 1457(s), 1374(m), 1302(w), 1106(w), 1041 (vw), 947 (vw), 890 (vw), 717 cm^{-1} (m).

[1] Y.-F. Song, L. Cronin, *Angew. Chem.* **2008**, *120*, 4713–4715; *Angew. Chem. Int. Ed.* **2008**, *47*, 4635–4637.

[2] H. Chae, D. Y. Siberio-Perez, J. Kim, Y. Go, M. Eddaoudi, A. Matzger, M. O'Keeffe, O. M. Yaghi, *Nature* **2004**, *427*, 523–527.

[3] Z. Wang, S. M. Cohen, *Angew. Chem.* **2008**, *120*, 4777–4780; *Angew. Chem. Int. Ed.* **2008**, *47*, 4699–4702; D. Bradshaw, J. E. Warren, M. J. Rosseinsky, *Science* **2007**, *315*, 977–980.

[4] C. Serre, C. Mellot-Draznieks, S. Surble, N. Audebrand, Y. Filinchuk, G. Férey, *Science* **2007**, *315*, 1828–1831.

[5] N. S. Oxtoby, A. J. Blake, N. R. Champness, C. Wilson, *Proc. Natl. Acad. Sci. USA* **2002**, *99*, 4905–4910.

[6] S. Hasegawa, S. Horike, R. Matsuda, S. Furukawa, K. Mochizuki, Y. Kinoshita, S. Kitagawa, *J. Am. Chem. Soc.* **2007**, *129*, 2607–2614.

[7] H.-M. Yuan, J.-S. Chen, G.-S. Zhu, J.-Y. Li, J.-H. Yu, G.-D. Yang, R.-R. Xu, *Inorg. Chem.* **2000**, *39*, 1476–1479.

[8] S.-H. Cho, B. Ma, S. T. Nguyen, J. T. Hupp, T. E. Albrecht-Schmitt, *Chem. Commun.* **2006**, 2563–2566.

[9] H. J. Choi, M. P. Suh, *J. Am. Chem. Soc.* **2004**, *126*, 15844–15851.

[10] D.-L. Long, E. M. Burkholder, L. Cronin, *Chem. Soc. Rev.* **2007**, *36*, 105–121; S. G. Mitchell, C. Ritchie, D.-L Long, L. Cronin, *Dalton Trans.* **2008**, 1415–1417.

[11] C. P. Pradeep, D.-L. Long, G. N. Newton, Y. Song, L. Cronin, *Angew. Chem.* **2008**, *120*, 4460–4463; *Angew. Chem. Int. Ed.* **2008**, *47*, 4388–4391.

[12] Y. Song, D.-L. Long, L. Cronin, *Angew. Chem.* **2007**, *119*, 3974–3978; *Angew. Chem. Int. Ed.* **2007**, *46*, 3900–3904.

[13] C. Ritchie, E. M. Burkholder, D. Adam, D.-L. Long, P. Kögerler, L. Cronin, *Chem. Commun.* **2006**, 468–470.

[14] A family of isostructural materials has been synthesized where M = manganese or cobalt, and X = silicon or germanium.

[15] J. Canny, A. Tézé, R. Thouvenot, G. Hervé, *Inorg. Chem.*, **1985**, *25*, 2114–2119..

[16] Crystal data and structure refinement for 1_{ox}: [C$_{160}$H$_{496}$N$_{40}$Mn$_{12}$O$_{356}$Si$_7$W$_{72}$], M_r = 22770 g mol^{-1}; a tetrahedral brown crystal (0.18 × 0.15 × 0.15 mm^3) was analyzed with a Rigaku Image Plate diffractometer using Mo$_{K\alpha}$ radiation (λ = 0.71073 Å) at 150(2) K. Cubic, space group I$\bar{4}$3d, a = 38.541(5) Å, V = 57249(12) Å^3, Z = 4, ρ = 2.631 g cm^{-3}, μ-(Mo$_{K\alpha}$) = 14.757 mm^{-1}, $F(000)$ = 41240, 30628 reflections measured, of which 6229 are independent, 364 refined parameters, $R1$ = 0.0829, $wR2$ = 0.2010. Many data sets were collected of the native material, and the material returned to the oxidized state during the redox cycles and the average unit cell parameter was 38.54(4) with a maximum variation of (± 0.02) Å. Crystal data and structure refinement for 1_{red}: [C$_{160}$H$_{508}$Mn$_{12}$N$_{40}$O$_{356}$Si$_7$W$_{72}$], M_r = 22782 g mol^{-1}; a yellow tetrahedral crystal (0.18 × 0.16 × 0.16 mm^3) was analyzed with an Oxford Diffraction Gemini Ultra diffractometer using Mo$_{K\alpha}$ radiation (λ = 0.71073 Å) at 150(2) K. Cubic, space group I$\bar{4}$3d, a = 39.2325(5) Å, V = 60386.2(13) Å^3, Z = 4, ρ = 2.501 g cm^{-3}, μ(Mo$_{K\alpha}$) = 13.991 mm^{-1}, $F(000)$ = 41288, 105212 reflections measured, of which 4692 are independent, 352 refined parameters, $R1$ = 0.0768, $wR2$ = 0.1596. Many data sets were collected during the redox cycles and the average unit cell parameter was 39.21(4) with a maximum variation of 0.02. CCDC 666402 (1_{ox}) and CCDC 666403 (1_{red}) contain the supplementary crystallographic data for this paper. These data can be obtained free of charge from The Cambridge Crystallographic Data Centre via www.ccdc.cam.ac.uk/data_request/cif.

[17] M. I. Khan, E. Yohannes, R. J. Doedens, *Angew. Chem.* **1999**, *111*, 1374–1376; *Angew. Chem. Int. Ed.* **1999**, *38*, 1292–1294.

[18] C. Pichon, A. Dolbecq, P. R. Mialane, J. Marrot, E. Rivière, F. Sécheresse, *Dalton Trans.* **2008**, 71–76.

[19] P. Kroll, *J. Solid State Chem.* **2003**, *176*, 530–537.

[20] G. M. Tsivgoulis, P. A. Afroudakis, P. V. Ioannou, *J. Inorg. Biochem.* **2004**, *98*, 649–656.